Polymer Chemistry

Accepted Manuscript

This is an *Accepted Manuscript*, which has been through the Royal Society of Chemistry peer review process and has been accepted for publication.

Accepted Manuscripts are published online shortly after acceptance, before technical editing, formatting and proof reading. Using this free service, authors can make their results available to the community, in citable form, before we publish the edited article. We will replace this *Accepted Manuscript* with the edited and formatted *Advance Article* as soon as it is available.

You can find more information about *Accepted Manuscripts* in the Information for Authors.

Please note that technical editing may introduce minor changes to the text and/or graphics, which may alter content. The journal's standard Terms & Conditions and the Ethical guidelines still apply. In no event shall the Royal Society of Chemistry be held responsible for any errors or omissions in this *Accepted Manuscript* or any consequences arising from the use of any information it contains.

ROYAL SOCIETY OF CHEMISTRY

www.rsc.org/polymers

Journal Name

ARTICLE

Poly(Pentacyclic Lactam-alt-Diketopyrrolopyrrole) for Field-Effect Transistors and Polymer Solar Cells Processed from Non-Chlorinated Solvents

Received 00th January 20xx,
Accepted 00th January 20xx

DOI: 10.1039/x0xx00000x

www.rsc.org/

Guitao Feng,[a,b] Yunhua Xu,[a] Chengyi Xiao,[b] Jianqi Zhang,[c] Xiaotao Zhang,*[b,d] Cheng Li,*[b] Zhixiang Wei,[c] Wenping Hu,[b,d] Zhaohui Wang[b] and Weiwei Li*[b]

A semi-crystalline conjugated polymer based on two electron-deficient units, pentacylic lactam (PCL) and diketopyrrolopyrrole (DPP), was designed and synthesized for the application in field-effect transistors (FETs) and polymer solar cells (PSCs). The polymer performs high molecular weight, near-infrared absorption up to 900 nm and good solubility in toluene. When the polymer thin films were solution-processed from toluene with diphenyl ether as additive, FET devices achieved high hole mobility of 0.81 $cm^2 V^{-1} s^{-1}$. With the same solution-processing solvents, bulk-heterojunction solar cells based on this polymer as electron donor provided power conversion efficiency of 4.7% with optimal energy loss of 0.65 eV due to its deep lowest unoccupied molecular orbital level. Further study on the morphology of pure polymer or blend thin films by atom force microscopy, transmission electron microscopy and 2D- grazing-incidence wide angle X-ray scattering reveals that the new polymer has good crystalline property, which is mainly due to its coplanar nature of conjugated backbone. The study in this work demonstrates that conjugated polymers incorporating several electron-deficient units can be potential used in high performance FETs and PSCs.

Introduction

There is considerable interest in designing conjugated polymers incorporating multiple electron-deficient units into the main chain for application in organic field-effect transistors (FETs)[1-10] and polymer solar cells (PSCs)[11-16] in recent years. These polymers have the regularly alternated structures of electron-deficient moieties that allow for tuning the optical band gap and frontier energy levels. The transistors based on these polymers show ambipolar1-23[4] or n-type properties.[5-6789][10] Meanwhile, these polymers as electron donor[11,12] or electron acceptor[13-16] have been successfully applied in bulk-heterojunction solar cells.

Conjugated polymers that comprise electron-rich and electron-deficient units in the conjugated backbone represent the most successful materials to realize high performance thin film transistors and photovoltaics.[17 - 20] Electron-rich units mainly determine the highest occupied molecular orbital (HOMO) levels and electron-deficient units relate to the lowest unoccupied molecular orbital (LUMO) levels, which together lower the band gap of conjugated polymers by intra-molecular charge transfer in the main chain. When introducing two kinds of electron-deficient units into one polymer, the corresponding polymer prefers low-lying LUMO level, which is beneficial for n-type FET devices. Conjugated polymers with deep LUMO levels can also be applied as non-fullerene acceptor for polymer-polymer solar cells.[21] In addition, the electron-withdrawing main chains tend to stabilize the quinoid resonance structure along the conjugated backbone, resulting in good charge generation and transportation in organic electronics.

Herein, two electron-deficient units, pentacylic lactam (PCL)[22-25] and diketopyrrolopyrrole (DPP),[26-28] are applied into one conjugated polymer for FETs and PSCs. Both PCL and DPP units have the imide groups that generate hydrogen bonds or other electrostatic interactions, resulting in ordered and crystalline polymers. PCL based conjugated polymers have exhibit high power conversion efficiency (PCEs) over 9% with photoresponse to 700 nm in PSCs.[25] DPP unit has strong electron-withdrawing ability so that DPP-based polymers perform near-infrared absorption up to 1000 nm.[29] DPP polymers have shown high hole,[30-35] ambipolar1'2'[36,37] and electron mobilties[38-41] > 1 $cm^2 V^{-1} s^{-1}$ in FET devices. PSCs with DPP polymers as electron donor have realized PCEs over 8%.[42-45] Therefore, it will be interesting to explore conjugated polymers that combine with PCL and DPP units.

[a] Department of Chemistry, School of Science, Beijing Jiaotong University, Beijing 100044, China.
[b] Beijing National Laboratory for Molecular Sciences, CAS Key Laboratory of Organic Solids, Institute of Chemistry, Chinese Academy of Sciences, Beijing 100190, China. E-mail: zhangxt@iccas.ac.cn, licheng1987@iccas.ac.cn, liweiwei@iccas.ac.cn.
[c] National Center for Nanoscience and Technology, Chinese Academy of Sciences, Beijing 100190, China.
[d] Department of Chemistry, School of Science, Tianjing University, Tianjin 300072, China
† Electronic Supplementary Information (ESI) available. See DOI: 10.1039/x0xx00000x

The new polymer PDPP2TPCL (Scheme 1) exhibits high molecular weight, narrow band gap and good planarity. Interestingly, PDPP2TPCL shows good solubility in toluene, indicating that the organic electronic devices can be fabricated from non-chlorinated solvents. PDPP2TPCL based bottom gate – bottom contact (BGBC) configuration FETs presents a hole mobility of 0.78 cm^2 V^{-1} s^{-1} when solution-processed from toluene with diphenyl ether (DPE) as additive. With the same solvent, PSCs based on PDPP2TPCL as electron donor provide PCEs of 4.7% with photoresponse up to 900 nm. Atom force microscopy (AFM), transmission electron microscopy (TEM) and 2-D grazing-incidence wide angle X-ray scattering (2D-GIWAXS) reveals that PDPP2TPCL has the strong tendency to form crystalline structures in thin films, which is responsible for its good performance in FETs and PSCs. Our results demonstrate that the conjugated polymers with electron-deficient PCL and DPP units can realize narrow band gap and strong crystallinity, which are potentially used as electron donor for high performance organic electronic devices.

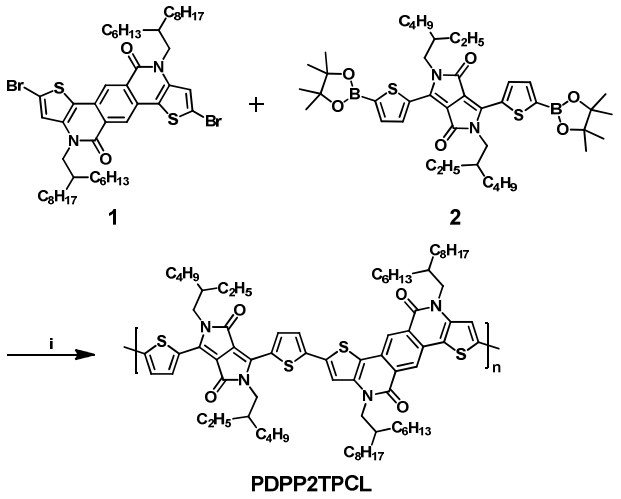

Scheme 1 Chemical structure of the DPP polymer PDPP2TPCL and its synthetic route. (i) Suzuki polymerization by using Pd_2dba_3/(t-Bu)$_3$PH[BF_4]/K_3PO_4 (aq)/Aliquat 336 in THF at 80 °C.

Experimental

Materials and Measurements

All synthetic procedures were performed under argon atmosphere. Commercial chemicals were used as received. THF and toluene were distilled from sodium under an N_2 atmosphere. [6,6]-phenyl-C61-butyric acid methyl ester ([60]PCBM) was purchased from Solarmer Materials Inc. 2,8-dibromo-4,10-bis(2-hexyldecyl)-4,10-dihydrothieno[2',3':5,6]pyrido[3,4-*g*]thieno[3,2-*c*]isoquinoline-5,11-dione (1)[22] and 2,5-bis(2-ethylhexyl)-3,6-bis(5-(4,4,5,5-tetramethyl-1,3,2-dioxaborolan-2-yl)thiophen-2-yl)-2,5-dihydropyrrolo[3,4-*c*]pyrrole-1,4-dione (2)[46] were synthszied according to literature procedures.

^{1}H-NMR and ^{13}C-NMR spectra were recorded at 400 MHz and 100 MHz on a Bruker ANACE spectrometer with $CDCl_3$ as the solvent and tetramethylsilane (TMS) as the internal standard. Molecular weight was determined with GPC at 140 °C on a PL-GPC 220 system using a PL-GEL 10 μm MIXED-B column and *o*-DCB as the eluent againt polystyrene standards. Low concentration of 0.1 mg mL^{-1} polymer in *o*-DCB was applied to reduce aggregation. Electronic spectra were recorded on a JASCO V-570 spectrometer. Cyclic voltammetry was conducted with a scan rate of 0.1 V s^{-1} under an inert atmosphere with 1 M tetrabutylammonium hexafluorophosphate in *o*-DCB as the electrolyte. The working, counter and reference electrodes were glassy carbon, Pt wire and Ag/AgCl, respectively. The concentration of the sample in the electrolyte was approximately 1 mM, based on monomers. All potentials were corrected against Fc/Fc^+. Density function theory (DFT) calculations were performed at the B3LYP/6-31G* level of theory by using the Gaussian 09 program package. AFM images were recorded using a digital instruments nanoscope IIIa multimode atomic force microscope in tapping mode. Bright field TEM images were performend on a Hitachi SU8200 scanning electron microscope. Grazing-incidence wide-angle X-ray Scattering (GIWAXS) measurements were conducted on Xenocs-SAXS/WAXS system with X-ray wavelength of 1.5418 Å. The film samples were irradiated at a fixed angle of 0.2°. All film samples are prepared by spin-coating solutions on Si/SiO_2 substrate.

The organic field-effect transistors were fabricated on a commercial Si/SiO_2/Au substrate purchased from First MEMS Co. Ltd. A heavily N-doped Si wafer with a SiO_2 layer of 300 nm served as the gate electrode and dielectric layer, respectively. The Ti (2 nm)/Au (28 nm) source–drain electrodes were sputtered and patterned by a lift-off technique. Before deposition of the organic semiconductor, the gate dielectrics were treated with octadecyltrichlorosilane (OTS) in a vacuum oven at a temperature of 120 °C, forming an OTS self-assembled monolayers. The treated substrates were rinsed successively with hexane, chloroform ($CHCl_3$), and isopropyl alcohol. Polymer thin films were spin coated on the substrate from solution with a thickness of around 30 – 50 nm. The polymer thin films were solution-processed from $CHCl_3$ solution at room temperature, while the toluene solution with or without DPE as additive was heated to 90 °C for hot spin coating. The devices were thermally annealed at 120 °C on the hotplate for 10 min in a glovebox filled with N_2. The devices were measured on an Keithley 4200 SCS semiconductor parameter analyzer at room temperature. The mobilities were calculated from the saturation region with the following equation: $I_{DS} = (W/2L)C_i\mu(V_G-V_T)^2$, where I_{DS} is the drain–source current, W is the channel width (1400 μm), L is the channel length (50 μm), μ is the field-effect mobility, C_i is the capacitance per unit area of the gate dielectric layer, and V_G and V_T are the gate voltage and threshold voltage, respectively. This equation defines the important characteristics of electron mobility (μ), on/off ratio (I_{on}/I_{off}), and threshold voltage (V_T), which could be deduced by the equation from the plot of current–voltage.

Photovoltaic devices with inverted configuration were made by spin-coating a ZnO sol-gel[47] at 4000 rpm for 60 s onto pre-

cleaned, patterned ITO substrates. The photoactive layer was deposited by spin coating a chloroform (or toluene) solution containing DPP polymers and [60]PCBM and the appropriate amount of processing additive such as DIO, *o*-DCB, or DPE in air. The toluene solution was heated to 90 °C for hot spin coating. MoO_3 (10 nm) and Ag (100 nm) were deposited by vacuum evaporation at ca. 4×10^{-5} Pa as the back electrode.

The active area of the cells was 0.04 cm^2. The *J-V* characteristics were measured by a Keithley 2400 source meter unit under AM1.5G spectrum from a solar simulator (Enlitech model SS-F5-3A). Solar simulator illumination intensity was determined at 100 mW cm^{-2} using a monocrystal silicon reference cell with KG5 filter. Short circuit currents under AM1.5G conditions were estimated from the spectral response and convolution with the solar spectrum. The external quantum efficiency was measured by a Solar Cell Spectral Response Measurement System QE-R3011 (Enli Technology Co., Ltd.). The thickness of the active layers in the photovoltaic devices was measured on a Veeco Dektak XT profilometer.

PDPP2TPCL

To a degassed solution of monomer **1** (88.72 mg, 95.3 μmol), monomer **2** (74.01 mg, 95.3 μmol) in THF (4 mL) and H_2O (1 mL) contained 2M K_3PO_4, tris(dibenzylideneacetone)dipalladium(0) (2.62 mg, 2.86 μmol) and tri-tert-butylphosphonium tetrafluoroborate (3.32 mg, 11.4 μmol) were added. The mixture was stirred at 80 °C for overnight, after which it was precipitated in methanol and filter through a Soxhlet thimble. The polymer was extracted with acetone, hexane and chloroform. The chloroform fraction was reduced and the polymer was precipitated in acetone. The polymer was collected by filtering over a 0.45 µm PTFE membrane filter and dried in a vacuum oven to yield PDPP2TPCL (116.3 mg, 94%) as a dark solid. GPC (*o*-DCB, 140 °C): M_n = 72.8 kg mol^{-1}, M_w = 239.9 kg mol^{-1} and PDI = 3.3.

Results and discussion

Synthesis

The synthesis procedure for the polymer PDPP2TPCL is shown in Scheme 1. The monomer 2,8-dibromo-4,10-bis(2-hexyldecyl)-4,10-dihydrothieno[2',3':5,6]pyrido[3,4-*g*]thieno[3,2-*c*]isoquinoline-5,11-dione (1) and 2,5-bis(2-ethylhexyl)-3,6-bis(5-(4,4,5,5-tetramethyl-1,3,2-dioxaborolan-2-yl)thiophen-2-yl)-2,5-dihydropyrrolo[3,4-*c*]pyrrole-1,4-dione (2) was used to synthesis PDPP2TPCL via Suzuki polymerization, where the catalyst of Pd_2dba_3 and the ligand of tri-tert-butylphosphonium tetrafluoroborate ($(t\text{-}Bu)_3PH[BF_4]$) was applied to achieve a high molecular weight. The new polymer shows good solubility in chloroform ($CHCl_3$) at room temperature, and is dissolved in dichlorobenzene (*o*-DCB) or toluene at 90 °C. After cooling to room temperature, the polymer solution in toluene formed gel-like structures in 2 min. The molecular weight of the polymer was determined by gel permeation chromatography (GPC) with *o*-DCB as eluent at 140 °C, as shown in the supporting information (ESI†) Fig. S1. PDPP2TPCL shows a high number molecular weight (M_n) of 72.8 kg mol^{-1} and PDI of 3.3, which is comparable to other DPP polymers.[48]

Optical and electrochemical properties

UV-vis absorption spectra of the polymer PDPP2TPCL in $CHCl_3$ and thin films are present in Fig. 1a. The polymer shows the absorption peak at ≈ 760 nm with onset at 847 nm. Compared to dilute solution, the polymer shows a bathochromic shift absorption in solid-state film as a result of aggregation. The optical band gap of PDPP2TPCL is 1.42 eV, determined by the absorption onset at 873 nm in the thin film.

The HOMO and LUMO energy levels of PDPP2TPCL were determined by cyclic voltammetry (CV) measurements and are referenced to a work function of ferrocene of -5.23 eV (Fig. 1b). The polymer shows LUMO and HOMO levels of -3.89 eV and -5.06 eV, which provides the LUMO offset of 0.27 eV between the polymer and PCBM.[49] This offset is close to 0.30 eV that is generally accepted as minimum driving force for the efficient exciton separation into free charges.[50] Recently, some researches also reveal that charge separation is also occurred when LUMO offset is below 0.30 eV,[51,52] indicating that PDPP2TPCL can be potentially as electron donor for PSCs.

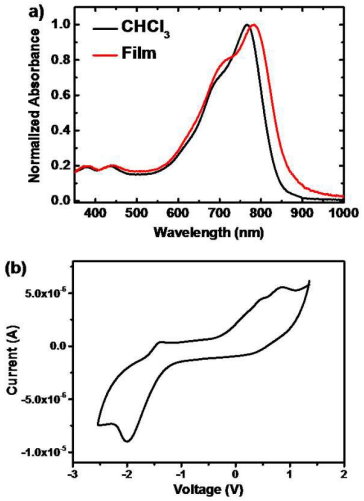

Fig. 1 (a) optical absorption spectra of PDPP2TPCL in $CHCl_3$ solution (black line) and in solid state films (red line). (b) Cyclic voltammograms of PDPP2TPCL thin film. Potential vs. Fc/Fc^+.

DFT-calculated molecular geometries and orbitals

To study the effect on electron-deficient PCL and DPP units on the frontier orbitals over the conjugated backbone, density functional theory (DFT) calculations were carried out on oligomers PCL-TDPPT-PCL-TDPPT (Fig. 2). The polymer exhibits the coplanar backbone with very small torsion angles, which is helpful to form crystalline structures in polymer thin films (Fig. 2a and b). The polymer has more localized HOMO and LUMO levels on the DPP-segments, which indicate that strong electron-deficient DPP units have more impact on the energy levels of the polymer (Fig. 2c and d). The high molecular

weight, narrow band gap and coplanar backbone are beneficial for charge transport in FETs and PSCs.

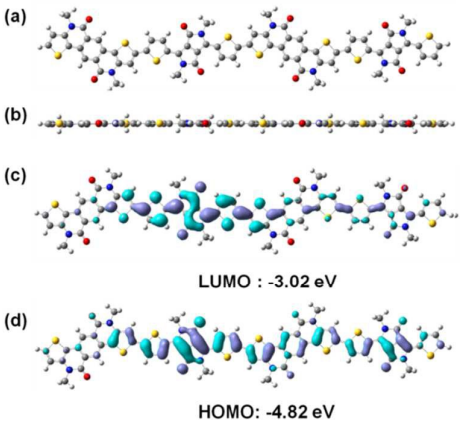

Fig. 2 DFT calculations of the segment of PCL-TDPPT-PCL-TDPPT. (a) front view and (b) side view of optimized molecular geometric. (c) and (d) frontier molecular orbitals.

Charge carrier mobility

The polymer PDPP2TPCL was applied in FETs with a BGBC configuration. The silicon dioxide gate dielectric used was passivated with octadecyltrichlorosilane (OTS). The polymer thin films were solution-processed from $CHCl_3$ or toluene without or with DPE as additive and thermally annealed for 10 min at 120 °C before measurement. The FET devices from the polymer thin films without or with thermal annealing at 100 °C or 150 °C (Table S1) showed low hole mobilities compared to those films thermal annealed at 120 °C (Table 1).

The hole mobility of the polymer spin coated from $CHCl_3$ solution were measured to be 0.48 $cm^2\ V^{-1}\ s^{-1}$ (Fig. S2a and b, ESI†, Table 1). When the polymer thin film was spin coated from toluene solution, the hole mobility was slightly decreased to 0.35 $cm^2\ V^{-1}\ s^{-1}$ (Fig. S2c and d, ESI†, Table 1). The hole mobility was increased to 0.81 $cm^2\ V^{-1}\ s^{-1}$ after adding high boiling point DPE as additive into the polymer solution in toluene. FET devices fabricated from these solutions provided similar threshold voltage (V_T) and on/off ratio (Table 1).

The difference of hole mobilities of PDPP2TPCL spin coated from different solvents was further analyzed by atom force microscopy (AFM) (Fig. 3c and d, Fig. S3, ESI†). AFM images clearly show the fibril-like structures in these thin films, indicating the strong crystalline properties of PDPP2TPCL. In addition, the polymer thin films processed from toluene/DPE show larger crystal domain than those from $CHCl_3$ and toluene, which is further confirmed by its high roughness (3.02 nm) compared to the thin films from $CHCl_3$ and toluene (0.87 nm and 0.88 nm) (Fig. S3, ESI†).

It is interesting to mention that electron mobilities are too low to be observed in these BGBC FET devices, although the polymer PDPP2TPCL also has LUMO level of -3.89 eV. We further apply top gate – bottom contact (TGBC) configuration with polymethylmethacrylate (PMMA) as dielectric layer to fabricate PDPP2TPCL based transistors (ESI† for detailed experimental procedures). The electron mobilties were much lower than the hole mobilties (Figure S4 and Table S2, ESI†). The low electron mobilities of the polymer PDPP2TPCL are probably due to relative high-lying LUMO level, the aggregation of the polymer thin films and environmental influence such as H_2O and O_2.

Table 1 Field-effect hole mobilities of PDPP2TPCL thin films in a BGBC configuration. The polymer thin films were thermal annealed at 120 °C for 10 min before measurement.

solvent	μ_h [$cm^2\ V^{-1}\ s^{-1}$]	V_T [V]	I_{on}/I_{off}
$CHCl_3$	0.48	-7.1	1×10^4
Toluene	0.35	-9.6	1×10^4
Toluene/DPE (2%)	0.81	-7.6	7×10^4

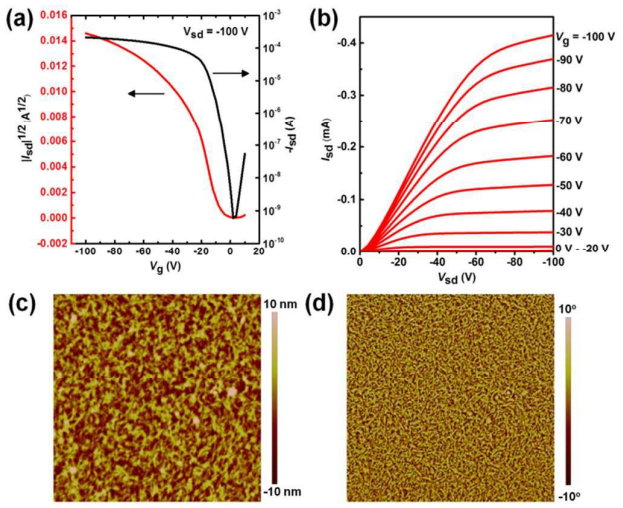

Fig. 3 (a) Transfer and (b) output curves obtained from BGBC FETs device with PDPP2TPCL thin film processed from toluene/DPE solution and annealed at 120 °C. (c) AFM height image (3×3 μm^2) and (d) phase image of the corresponding thin film. The RMS roughness is 3.02 nm.

Photovoltaic properties

The polymer PDPP2TPCL was further applied as electron donor in bulk-heterojunction photovoltaic cells when blending with phenyl-C_{61}-butyric acid methyl ester ([60]PCBM) as electron acceptor in an inverted device configuration with an ITO/ZnO electrode for electron collection and a MoO_3/Ag electrode for hole collection. The photoactive layers were carefully optimized with respect to the solution processing solvent, high boiling point additive, the donor to acceptor ratio and the thickness of the active layers (Table S3-S5, Fig. S5-S7, ESI†). The optimized polymer:PCBM weight ratio is 1:3. The *J-V* characteristics and external quantum efficiency (EQE) for the optimized solar cells are shown in Fig. 4 and Table 2. Short circuit current density (J_{sc}) was determined by integrating the EQE with the AM1.5G spectrum.

Initially, PDPP2TPCL:PCBM cells have a PCE of 3.4% with J_{sc} = 6.7 mA cm^{-2}, open circuit voltage (V_{oc}) of 0.77 V and a high fill factor (FF) of 0.66 when the active layers were spin coated from $CHCl_3$ with 2% DPE as additive (Table 2). The PCE of PDPP2TPCL:PCBM cells was dramatically increased to 4.7% when using toluene with 2% DPE as additive, which is mainly

due to the high J_{sc} of 9.5 mA cm^{-2}. These two cells show a broad photoresponse from 300 nm to 900 nm (Fig. 4b). The cells processed from $CHCl_3$/DPE provide the maximum external quantum efficiency (EQE) of 0.30 at 795 nm, whereas the EQE of the cells from toluene/DPE increases to 0.44. The high EQE also explains the increased J_{sc}. It is also noted that the energy loss of PDPP2TPCL:PCBM cells, defined as the difference between optical band gap and V_{oc}, is 0.65 eV that is close to the onset of 0.6 eV.[51] The low energy loss, that is used to enhance the performance of photovoltaic devices, can be realized via deep LUMO levels of the donor polymers. Therefore, the acceptor-acceptor polymers with low-lying LUMO levels have the potential to realize high performance PSCs.

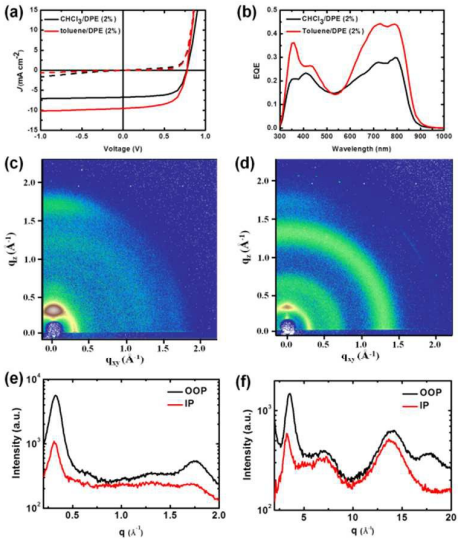

Fig. 4 (a) *J-V* characteristics in dark (dashed lines) and under white light illumination (solid lines). (b) EQE of the optimized polymer:[60]PCBM (1:3) inverted solar cells fabricated from $CHCl_3$/DPE or toluene/DPE solution. 2D-GIWAXS patterns of the thin films spin coated from toluene/DPE (2%). (c) PDPP2TPCL and (d) PDPP2TPCL:[60]PCBM (1:3). The out-of-plane (OOP) and in plane (IP) cuts of the corresponding 2D-GIWAXS patterns. (e) PDPP2TPCL and (f) PDPP2TPCL:[60]PCBM.

Table 2 Solar cell parameters of optimized solar cells of PDPP2TPCL:[60]PCBM (1:3).

solvent	Thickness [nm]	J_{sc}[a] [mA cm^{-2}]	V_{oc} [V]	FF	PCE [%]
$CHCl_3$/DPE (2%)	100	6.7	0.77	0.66	3.4
toluene/DPE (2%)	120	9.5	0.77	0.64	4.7

[a] J_{sc} as calculated by integrating the EQE spectrum with the AM1.5G spectrum. Ratio of donor to acceptor is 1:3.

The photoactive layers were further studied by 2D-GIWAXS, AFM and TEM images (Fig. 4c – f and Fig. 5). PDPP2TPCL exhibits both (100) and (010) diffraction peaks in the out-of-plane direction, indicating that PDPP2TPCL polymer chains on the surface have no clear preference for "edge on" or "face on" orientation. The (100) diffraction peaks in PDPP2TPCL thin film with q = 0.32 Å^{-1} is correlated to the lamellar distance of d = 19.63 nm (Table 3), which is attributed to the stacking alkyl side chains of the polymer. The distinct (010) diffraction peak in the out-of-plane direction of the PDPP2TPCL evidences π-π stacking (spacing: ≈ 3.61 Å). When PDPP2TPCL is blended with PCBM, the (100) and (010) diffraction peaks in the out-of-plane direction are observed. Interestingly, the lamellar and π-π spacing is reduced to 17.95 Å and 3.51 Å (Table 3), indicating that the polymer in PDPP2TPCL:PCBM blend thin films has highly dense molecular packing.

Table 3 Crystallographic parameters of the polymer thin films from 2D-GIWAXS measurement.

	Lamellar spacing		π-π spacing	
	q [Å^{-1}]	d [Å]	q [Å^{-1}]	d [Å]
PDPP2TPCL	0.32	19.63	1.74	3.61
PDPP2TPCL:[60]PCBM[a]	0.35	17.95	1.79	3.51

[a] From GIWAXS patterns of the polymer:[60]PCBM films, the crystallographic parameters of [60]PCBM can also be calculated: q = 1.4 Å^{-1} and d = 4.49 Å. The polymer thin films were fabricated from toluene/DPE (2%) solutions.

The semi-crystalline properties of the PDPP2TPCL based thin films can also be observed in AFM and TEM images. As shown in AFM images (Fig. 5a and b), the PDPP2TPCL:PCBM thin film solution-processed from toluene/DPE clearly showed the fibrillar network. TEM images of the same thin films confirm that PDPP2TPCL present fibril-like nanostructures with a diameter of 10 – 20 nm, which provides the separated channels for charge transportation to the electrode. It is also noted that the diameter of fibrils is slightly larger than those of efficient DPP polymer-fullerene blend films (< 10 nm),[53] which would reduce the photocurrent and PCEs by preventing the exciton diffusion into the donor/acceptor interface to generate charges.

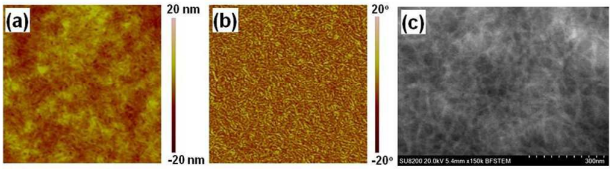

Fig. 5 (a) AFM height (3×3 μm^2), (b) phase and (c) TEM image of optimized PDPP2TPCL:[60]PCBM (1:3) spin coated from toluene/DPE (2%). The RMS roughness is 2.24 nm.

Conclusions

A new conjugated polymer based on two electron-deficient units of PCL and DPP was designed, synthesized and applied in FETs and PSCs. The polymer has high molecular weight, good solubility in toluene and narrow band gap of 1.42 eV. FETs based on the polymer thin films solution-processed from toluene with DPE as additive have hole mobilities of 0.81 cm^2 V^{-1} s^{-1}. With the same solvent, PSCs based on the polymer provide PCEs of 4.7% with a photoresponse up to 900 nm and low energy loss of 0.65 eV. The results demonstrate that acceptor-acceptor conjugated polymers can be as electron donors toward efficient FET and photovoltaic devices.

Acknowledgements

We thank Ralf Bovee and Qiang Wang at Eindhoven University of Technology (TU/e, Netherlands) for GPC analysis. This work was supported by the Recruitment Program of Global Youth Expertes of China. The work was further supported by the National Natural Science Foundation of China (21574138).

Notes and references

1 P. Sonar, S. P. Singh, Y. Li, M. S. Soh and A. Dodabalapur, *Adv. Mater.*, 2010, **22**, 5409-5413.
2 S. Cho, J. Lee, M. H. Tong, J. H. Seo and C. Yang, *Adv. Funct. Mater.*, 2011, **21**, 1910-1916.
3 J. D. Yuen, J. Fan, J. Seifter, B. Lim, R. Hufschmid, A. J. Heeger and F. Wudl, *J. Am. Chem. Soc.*, 2011, **133**, 20799-20807.
4 P. Wang, H. Li, C. Gu, H. Dong, Z. Xu and H. Fu, *RSC Adv.*, 2015, **5**, 19520-19527.
5 J.-K. Lee, M. C. Gwinner, R. Berger, C. Newby, R. Zentel, R. H. Friend, H. Sirringhaus and C. K. Ober, *J. Am. Chem. Soc.*, 2011, **133**, 9949-9951.
6 M. C. Gwinner, T. J. K. Brenner, J.-K. Lee, C. Newby, C. K. Ober, C. R. McNeill and H. Sirringhaus, *J. Mater. Chem.*, 2012, **22**, 4436-4439.
7 J. Lee, S. Cho, J. H. Seo, P. Anant, J. Jacob and C. Yang, *J. Mater. Chem.*, 2012, **22**, 1504-1510.
8 F. Grenier, P. Berrouard, J.-R. Pouliot, H.-R. Tseng, A. J. Heeger and M. Leclerc, *Polym. Chem.*, 2013, **4**, 1836-1841.
9 G. Kim, A. R. Han, H. R. Lee, J. Lee, J. H. Oh and C. Yang, *Chem. Commun.*, 2014, **50**, 2180-2183.
10 C. Ge, C. Mei, J. Ling, F. Zhao, H. Li, L. Liang, J. Wang, J. Yu, W. Shao, Y. Xie and W. Li, *J. Polym. Sci. Part A: Polym. Chem.*, 2014, **52**, 2356-2366.
11 K. Mahmood, H. Lu, Z.-P. Liu, C. Li, Z. Lu, X. Liu, T. Fang, Q. Peng, G. Li, L. Li and Z. Bo, *Polym. Chem.*, 2014, **5**, 5037-5045.
12 K. H. Hendriks, G. H. L. Heintges, M. M. Wienk and R. A. J. Janssen, *J. Mater. Chem. A*, 2014, **2**, 17899-17905.
13 C. Ge, C. Mei, J. Ling, J. Wang, F. Zhao, L. Liang, H. Li, Y. Xie and W. Li, *J. Polym. Sci. Part A: Polym. Chem.*, 2014, **52**, 1200-1215.
14 A. Zhang, C. Xiao, D. Meng, Q. Wang, X. Zhang, W. Hu, X. Zhan, Z. Wang, R. A. J. Janssen and W. Li, *J. Mater. Chem. C*, 2015, **3**, 8255-8261.
15 I. H. Jung, W.-Y. Lo, J. Jang, W. Chen, D. Zhao, E. S. Landry, L. Lu, D. V. Talapin and L. Yu, *Chem. Mater.*, 2014, **26**, 3450-3459.
16 I. H. Jung, D. Zhao, J. Jang, W. Chen, E. S. Landry, L. Lu, D. V. Talapin and L. Yu, *Chem. Mater.*, 2015, doi: 10.1021/acs.chemmater.5b01928.
17 M. Svensson, F. L. Zhang, S. C. Veenstra, W. J. H. Verhees, J. C. Hummelen, J. M. Kroon, O. Inganäs and M. R. Andersson, *Adv. Mater.*, 2003, **15**, 988-991.
18 Y. J. Cheng, S. H. Yang and C. S. Hsu, *Chem. Rev.*, 2009, **109**, 5868-5923.
19 H. Sirringhaus, *Adv. Mater.*, 2014, **26**, 1319-1335.
20 L. Dou, Y. Liu, Z. Hong, G. Li and Y. Yang, *Chem. Rev.*, 2015, DOI: 10.1021/acs.chemrev.5b00165.
21 A. Facchetti, *Mater Today*, 2013, **16**, 123-132.
22 J. Cao, Q. Liao, X. Du, J. Chen, Z. Xiao, Q. Zuo and L. Ding, *Energy Environ. Sci.*, 2013, **6**, 3224-3228.
23 Q. Liao, J. Cao, Z. Xiao, J. Liao and L. Ding, *Phys Chem Chem Phys*, 2013, **15**, 19990-19993.
24 C. Zuo, J. Cao and L. Ding, *Macromol. Rapid. Comm.*, 2014, **35**, 1362-1366.
25 H. Li, J. Cao, Q. Zhou, L. Ding and J. Wang, *Nano Energy*, 2015, **15**, 125-134.
26 Z. Yi, S. Wang and Y. Liu, *Adv. Mater.*, 2015, **27**, 3589-3606.
27 Y. Li, P. Sonar, L. Murphy and W. Hong, *Energy Environ. Sci.*, 2013, **6**, 1684-1710.
28 S. Y. Qu and H. Tian, *Chem. Commun.*, 2012, **48**, 3039-3051.
29 K. H. Hendriks, W. Li, M. M. Wienk and R. A. J. Janssen, *J. Am. Chem. Soc.*, 2014, **136**, 12130-12136.
30 P. Sonar, S. P. Singh, Y. N. Li, Z. E. Ooi, T. J. Ha, I. Wong, M. S. Soh and A. Dodabalapur, *Energy Environ. Sci.*, 2011, **4**, 2288-2296.
31 H. J. Chen, Y. L. Guo, G. Yu, Y. Zhao, J. Zhang, D. Gao, H. T. Liu and Y. Q. Liu, *Adv. Mater.*, 2012, **24**, 4618-4622.
32 Y. Li, P. Sonar, S. P. Singh, Z. E. Ooi, E. S. H. Lek and M. Q. Y. Loh, *Phys Chem Chem Phys*, 2012, **14**, 7162-7169.
33 I. Kang, H.-J. Yun, D. S. Chung, S.-K. Kwon and Y.-H. Kim, *J. Am. Chem. Soc.*, 2013, **135**, 14896-14899.
34 H. H. Choi, J. Y. Baek, E. Song, B. Kang, K. Cho, S.-K. Kwon and Y.-H. Kim, *Adv. Mater.*, 2015, **27**, 3626-3631.
35 J. Y. Back, H. Yu, I. Song, I. Kang, H. Ahn, T. J. Shin, S.-K. Kwon, J. H. Oh and Y.-H. Kim, *Chem. Mater.*, 2015, **27**, 1732-1739.
36 C. Xiao, G. Zhao, A. Zhang, W. Jiang, R. A. J. Janssen, W. Li, W. Hu and Z. Wang, *Adv. Mater.*, 2015, **27**, 4963-4968.
37 Z. Y. Chen, M. J. Lee, R. S. Ashraf, Y. Gu, S. Albert-Seifried, M. M. Nielsen, B. Schroeder, T. D. Anthopoulos, M. Heeney, I. McCulloch and H. Sirringhaus, *Adv. Mater.*, 2012, **24**, 647-652.
38 H.-J. Yun, S.-J. Kang, Y. Xu, S. O. Kim, Y.-H. Kim, Y.-Y. Noh and S.-K. Kwon, *Adv. Mater.*, 2014, **26**, 7300-7307.
39 B. Sun, W. Hong, Z. Yan, H. Aziz and Y. Li, *Adv. Mater.*, 2014, **26**, 2636-2642.
40 B. Sun, W. Hong, H. Aziz and Y. Li, *Polym. Chem.*, 2015, **6**, 938-945.
41 J. H. Park, E. H. Jung, J. W. Jung and W. H. Jo, *Adv. Mater.*, 2013, **25**, 2583-2588.
42 T. Ma, K. Jiang, S. Chen, H. Hu, H. Lin, Z. Li, J. Zhao, Y. Liu, Y.-M. Chang, C.-C. Hsiao and H. Yan, *Adv. Energy Mater.*, 2015, 10.1002/aenm.201501282.
43 H. Choi, S.-J. Ko, T. Kim, P.-O. Morin, B. Walker, B. H. Lee, M. Leclerc, J. Y. Kim and A. J. Heeger, *Adv. Mater.*, 2015, **27**, 3318-3324.
44 R. S. Ashraf, I. Meager, M. Nikolka, M. Kirkus, M. Planells, B. C. Schroeder, S. Holliday, M. Hurhangee, C. B. Nielsen, H. Sirringhaus and I. McCulloch, *J. Am. Chem. Soc.*, 2014, **137**, 1314-1321.
45 K. H. Hendriks, G. H. L. Heintges, V. S. Gevaerts, M. M. Wienk and R. A. J. Janssen, *Angew. Chem., Int. Ed.*, 2013, **52**, 8341-8344.
46 H. Bürckstümmer, A. Weissenstein, D. Bialas and F. Würthner, *J. Org. Chem.*, 2011, **76**, 2426-2432.
47 Y. M. Sun, J. H. Seo, C. J. Takacs, J. Seifter, A. J. Heeger, *Adv. Mater.,* 2011, **23**, 1679-1683.
48 W. Li, K. H. Hendriks, A. Furlan, W. S. C. Roelofs, M. M. Wienk and R. A. J. Janssen, *J. Am. Chem. Soc.*, 2013, **135**, 18942-18948.
49 M. M. Wienk, J. M. Kroon, W. J. H. Verhees, J. Knol, J. C. Hummelen, P. A. van Hal and R. A. J. Janssen, *Angew. Chem. Int. Ed.*, 2003, **42**, 3371-3375.
50 C. J. Brabec, C. Winder, N. S. Sariciftci, J. C. Hummelen, A. Dhanabalan, P. A. van Hal and R. A. J. Janssen, *Adv. Funct. Mater.*, 2002, **12**, 709-712.
51 W. Li, K. H. Hendriks, A. Furlan, M. M. Wienk and R. A. J. Janssen, *J. Am. Chem. Soc.*, 2015, **137**, 2231-2234.
52 K. Gao, L. Li, T. Lai, L. Xiao, Y. Huang, F. Huang, J. Peng, Y. Cao, F. Liu, T. P. Russell, R. A. J. Janssen and X. Peng, *J. Am. Chem. Soc.*, 2015, **137**, 7282-7285.
53 W. Li, K. H. Hendriks, A. Furlan, W. S. C. Roelofs, S. C. J. Meskers, M. M. Wienk and R. A. J. Janssen, *Adv. Mater.*, 2014, **26**, 1565-1570.

TOC Picture and text

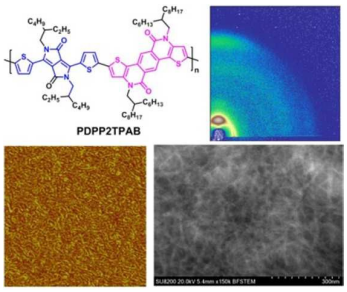

A highly crystalline conjugated polymer incorporating two electron-deficient units was applied in high performance organic field-effect transistors and polymer solar cells.